

DEFORMATION UNDER QUASI STATIC LOADING IN HIGH DENSITY POLYETHYLENE FILLED WITH NATURAL ZEOLITE

PURNOMO^{1,*}, R. SOENOKO², Y.S. IRAWAN², A. SUPRAPTO³

¹Department of Mechanical Engineering, Universitas Muhammadiyah Semarang, Indonesia

²Department of Mechanical Engineering, Brawijaya University, Malang, Indonesia

³Department of Mechanical Engineering, Merdeka University, Malang, Indonesia

*Corresponding Author: purnomo@unimus.ac.id

Abstract

This work aims to investigate the deformation under quasi static loading in zeolite-filled high density polyethylene. The investigation was carried out on dumbbell specimens by uniaxial tensile according to ISO 527 and on the double-edge-notched tension (DENT) specimens based on energy partitioning work of fracture. Energy partitioning approach, based on deformation mechanisms involved in the fracture process, is applied to DENT test to determine plane-stress fracture toughness. The test results showed that the composites with zeolite content of 20 wt.% on ligament length of 9, 10.5, and 15 mm indicated that they were not in plane stress state though initially had been configured in accordance with the requirements of plane stress conditions. This was due to the zeolite particles restricting the deformation which was parallel to specimen thickness in ligament region.

Keywords: Deformation, Quasi static, High density polyethylene, Zeolite.

1. Introduction

Biomaterials for implant are widely used to replace human organs and to correct abnormalities [1]. Recently, scientific research tends to develop polymer matrix composite for biomedical materials because these materials exhibit new alternative solutions for load-bearing components, such as skull reconstruction implant. The special character of the bone is the bone's fragility. It is difficult to deform when subjected to tensile stress or shear stress. In term of the elongation due to axial force, it tolerates a maximum deformation of 2% prior to fracture [2].

Biomaterial can behave plastically at large deformation that it can no longer perform its function. It depends on both the magnitude of the applied load and its

Nomenclatures	
l	Ligament length, mm
t	Specimen thickness, mm
W_e	Essential work for fracture, kJ/m^2
W_f	Total work required for fracture, kJ/m^2
W_p	Non-essential work, kJ/m^2
Greek Symbols	
β	Shape factor of the plastic region
γ	plastic constraint factor
σ_m	The mean value of σ_{max}
σ_{max}	Net section stress
σ_y	yield stress
Abbreviations	
ESIS	European Structural Integrity Society
ISO	International Standards Organization

duration. In other words, when the material deform beyond its elastic limit, the energy is sufficient to produce a fracture. Therefore, it is very important to learn the deformation of the biomaterial implants.

Zeolites are microporous aluminosilicate minerals that have been widely used in biomedical applications [3-6]. Some researchers have reported that zeolite is biocompatible and non-toxic [7, 8], and bioactive [9-12]. Moreover, zeolite is capable to prevent polymer matrix from degradation induced by exposure to ultra violet radiation [3] and it is found in abundance. All of the properties of zeolite that have been reported are potential filler in high density polyethylene (HDPE) as biomaterial for load-bearing implant such as skull reconstruction implant. HDPE that is biocompatible, inert, and stable in the human body [12-14] has been widely used as implant materials such as skull reconstruction implant [15, 16].

In this work, the deformation of the HDPE filled with zeolite for skull implant application was studied in quasi static conditions. The deformation was evaluated on dumbbell specimens under uniaxial tensile, and on DENT specimens based on energy partitioning work of plane-stress fracture. The elongation of DENT specimen was used to determine of crack opening displacement (COD), and then the work of fracture was calculated based on empirical relationship with COD.

2. Experimental

2.1. Material and composites production

Injection moulding grade of HDPE and natural zeolite were used in this study. The natural zeolite with a particle-size (PS) distribution range of $177 \leq \text{PS} < 250 \mu\text{m}$ (0.40 wt.%), $149 \leq \text{PS} < 177 \mu\text{m}$ (8.60 wt.%), $125 \leq \text{PS} < 149 \mu\text{m}$ (2.34 wt.%), $99 \leq \text{PS} < 125 \mu\text{m}$ (13.37 wt.%), $74 \leq \text{PS} < 99 \mu\text{m}$ (11.35 wt.%), and $\text{PS} < 74 \mu\text{m}$ (63.94 wt.%) was calcined at 300°C for 3 h using heating rate of $5^\circ\text{C}/\text{min}$. The HDPE powder that passed through a sieve with 60 mesh to the inch was mixed with calcined zeolite powder. The mixing was performed in dry conditions with zeolite weight of 5%,

10%, 10%, and 20%. After mixing, the blend powders were injection-molded into two shape of specimen test, *i.e.*, dumbbell and DENT specimens as shown in Fig. 1. For all blends, the injection parameters were set at barrel temperature of 160°C with holding time for about 2 minutes prior to injection.

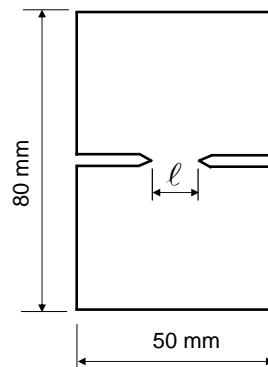


Fig. 1. Schematic of DENT sample used for essential work of fracture tests. Ligament length (l) was varied from 9 mm to 15 mm, and sample thickness (t) were nominally 3 mm.

2.2. Deformation investigation

2.2.1. Deformation measurement based on ISO 527 standard

The deformation by uniaxial tensile of zeolite/HDPE was investigated by tensile test on dumbbell shaped specimens. The tests were performed according to ISO 527 at room temperature under constant crosshead speed of 2 mm/min using a universal testing machine. All composites were given a tensile load to rupture and the elongation of the specimen tested was measured from the crosshead displacement of machine.

2.2.2. Deformation under essential work of fracture

The deformation under essential work of fracture (EWF) was obtained from the test of DENT specimens with dimension of 80 x 50 x 3 mm. To obtain the plane stress condition, in this work, the ligament length (l) was set within range of $3t$ - $5t$ [17-20], *i.e.*, 9-15 mm, where t is the specimen thickness. The tests were conducted at crosshead speed of 2 mm/min using universal testing machine at 25°C. During the test, deformation process was observed and recorded using SONY DCR-PJ6E. The results of the DENT test were analyzed based on the EWF concept. According to the EWF concept, total work required for fracture (W_f) of DENT specimen was divided into two parts: (i) the essential work for fracture (W_e) are carried in fracture process zone for the formation of new fracture surface, and (ii) the non-essential work (W_p), *i.e.*, the work for the plastic deformation. This concept can be expressed as [21-26]:

$$W_f = W_e + W_p \quad (1)$$

$$W_f = w_e \cdot t \cdot l + \beta \cdot w_p \cdot t \cdot l^2 \tag{2}$$

$$w_f = \frac{W_f}{t \cdot l} = w_e + \beta \cdot w_p \cdot l \tag{3}$$

where β is shape factor of the plastic region. The W_f is the area under the load-displacement curve and is obtained through the integration that curve. The specific essential work of fracture (w_e) which is failure work per unit surface area and specific non-essential work of fracture (βw_p) which is the plastic work per unit volume of plastic deformation zone are experimentally determined by plotting the specific fracture work (w_f) against ligament length. The fracture parameter w_e is the intercept on w_f at $l = 0$ and βw_p is the slope of linear fit extrapolation.

When the ligament region was fully yielded and crack initiated at the maximum load, followed by crack propagation with necking subsequent tearing until totally fracture, then the load-displacement curve was partitioned into two parts as shown in Fig. 2. Consequently, the W_f can be expressed as [19, 27]:

$$W_f = W_y + W_n \tag{4}$$

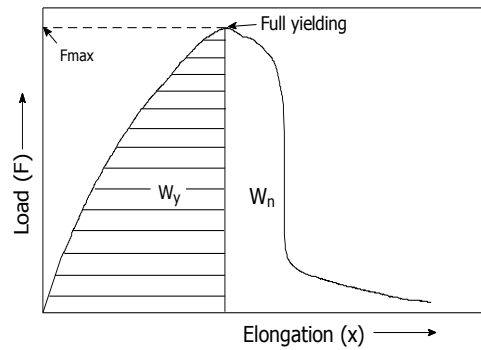


Fig. 2. Schematic explanation of energy partitioned EWF method [28].

where W_y is the total energy required for yielding (crack initiation) and W_n is total energy required for crack propagation (necking subsequent tearing). Consequently, parameters w_e and βw_p in Eq. (3) can be expressed in the following forms [19, 29, 30]:

$$w_e = w_{e,y} + w_{e,n} \tag{5}$$

$$\beta \cdot w_p = \beta_y \cdot w_{p,y} + \beta_n \cdot w_{p,n} \tag{6}$$

where $w_{e,y}$ and $w_{e,n}$ are specific essential for yielding (crack-initiating) work and necking subsequent tearing, respectively. The $w_{p,y}$ and $w_{p,n}$ are volumetric energy dissipated during yielding/crack initiation and necking subsequent tearing (crack propagation), respectively. The β_y and β_n are the shape factor related to form of plastic zone during yielding and necking subsequent tearing, respectively.

3. Results and Discussion

3.1. Uniaxial deformation according to test standard ISO 527

Various types of deformation are depicted in the experimental stress-strain curves for all composites and pure HDPE as shown in Fig. 3, which shows that the initial part of the plot is linear and the specimens behave in an elastic manner which means that specimens will restore to the original dimensions when the load is released and the slope of line in this region is appropriate for Young's modulus. Beyond the limit of proportionality, the specimens underwent extension will no longer be proportional to the load and are referred to as the yield point. Stress-strain behavior of pure HDPE shown in Fig. 3 depict that the strain in longitudinal direction of HDPE is higher than that of the composites which were decreased with increasing zeolite content.

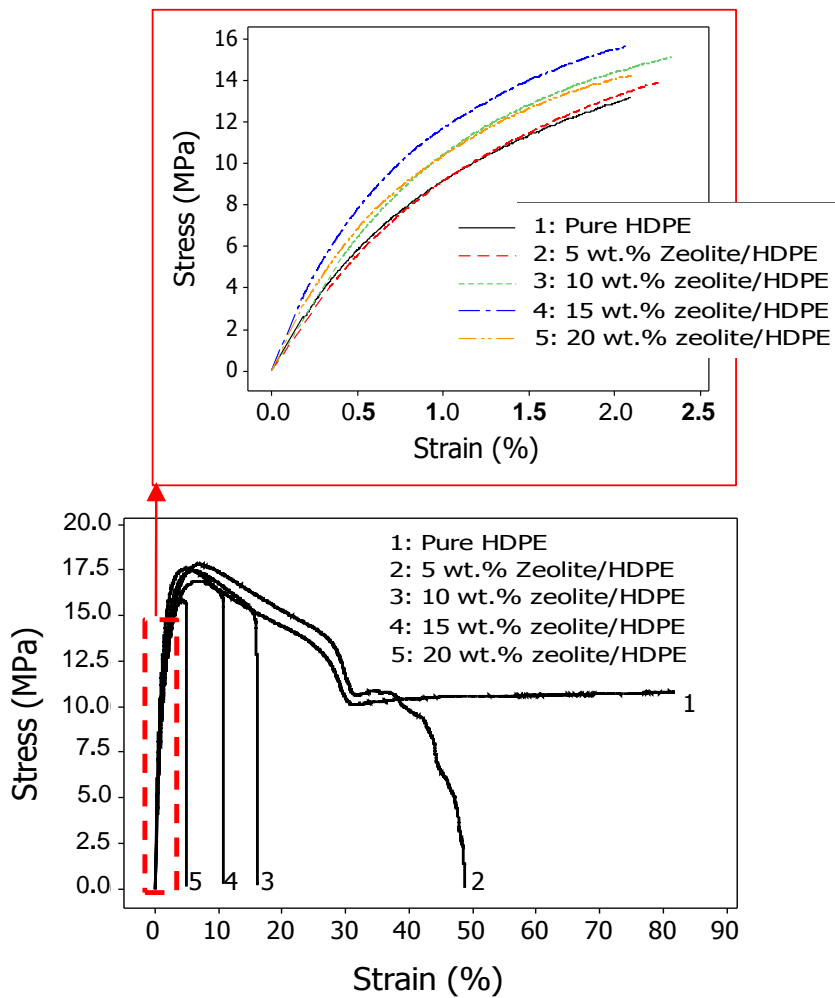


Fig. 3. Tensile stress-strain curve of dumbbell specimens.

3.2. Deformation mechanism under essential work of fracture process

The influence of zeolite content on load-displacement behavior (for ligament length of 15 mm) was presented in Fig. 4. It is clear that the incorporation of zeolite into HDPE causes gradual transition in the nature of the load-displacement curves characterized by a decrease in the maximum displacement. Apparently the elongation at break was reduced drastically which was indicated that the composites tended to become even more brittle in comparison to the composites with lower zeolite content and the pure HDPE.

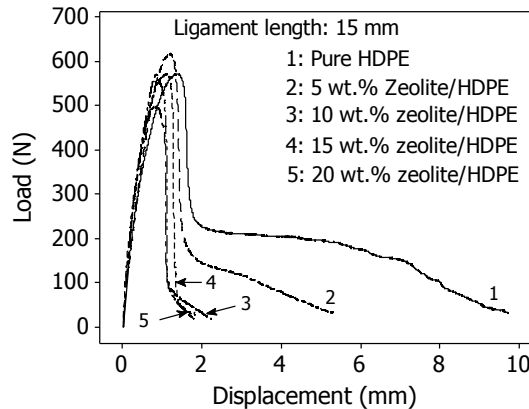


Fig. 4. The influence of zeolite content on load-displacement behavior.

It should be noted that all of DENT specimens have ligament length long meet the plane stress conditions. Furthermore, the fracture conditions were checked using the criteria proposed in the ESIS protocol [31] with the formula $0.9 < \sigma_{max} / \sigma_m < 1.1$, where σ_{max} is the net section stress while σ_m is the mean value of σ_{max} . The range values of σ_{max} on all zeolite content of composites were shown in Fig. 5. Not all composites were in plane stress fracture. In Fig. 5(e), the value of σ_{max} in ligament length of 9 and 10.5 mm were greater than $1.1 \sigma_m$, but on the other hand, σ_{max} in the ligament length of 15 mm was less than $0.9 \sigma_m$. Based on the criteria in the ESIS protocol [31], these composites were not in plane stress fracture despite their conformity with the criteria set by $(3-5)t \leq l \leq \min W/3$ [18, 19, 24, 25], where W was specimen width. It indicated that the composites were in flat surface perpendicular to the applied load and cannot deform laterally. Also, in that composites, the shear strain do not become operative mode of deformation.

To clarify the behavior of the deformation and fracture of HDPE in DENT test, a typical load-displacement curve (taken from a specimen of 5 wt.% zeolite/HDPE with $l = 15$ mm) is presented in Fig. 6. The typical load-displacement curve shows the change of load-drop rate during the whole fracture process. While, the image are views along the ligament length region taken from the front of the specimen at an angle of about 30 degrees, Figs. 6(a), (c), (e), (g), and (i), showing typical fracture development through the ligament, and side view, Figs. 6(b), (d), (f), (h) and (j) showing typical fracture development through the thickness of ligament length during DENT test.

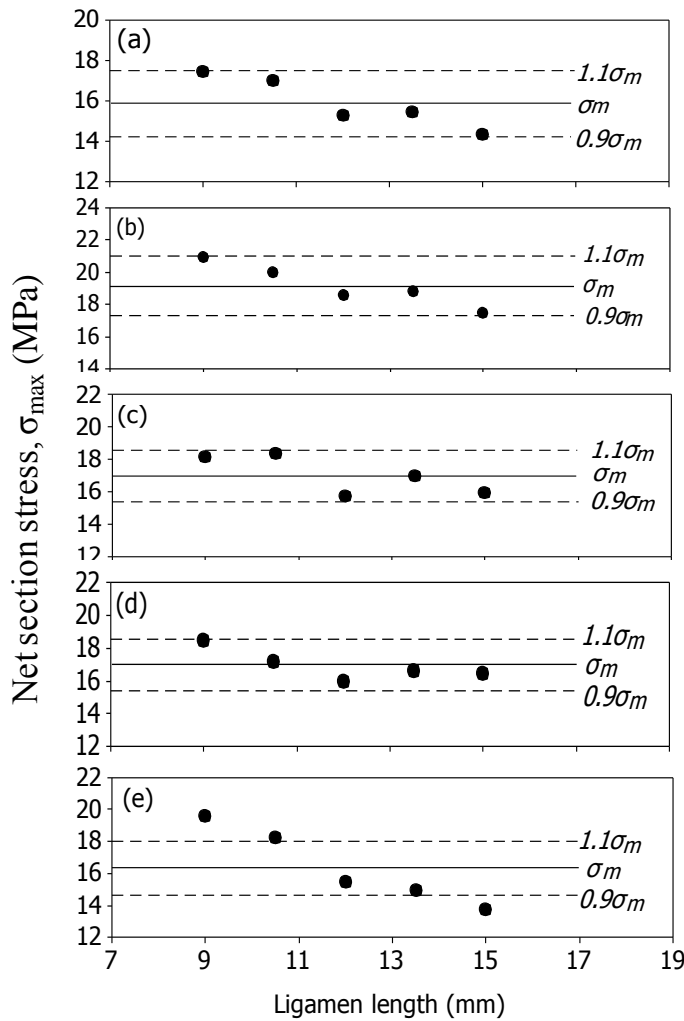


Fig. 5. Stress criteria according to ESIS protocol of EWF: (a) pure HDPE, (b) 5 wt.% zeolite/HDPE, (c) 10 wt.% zeolite/HDPE, (d) 15 wt.% zeolite/HDPE, and (e) 20 wt.% zeolite/HDPE.

When the maximum load achieved in the test, cracks initiated from both notch tips, furthermore the load drop due to the formation of fracture surface in the mid-thickness region. End stage of load dropping was reached when the two crack tips met each other in the middle section across the thickness, as shown by the image (g) and (h) in Fig. 6. Once the two cracks fully coalesced, the two halves of the DENT specimen were still connected by only the surface layer, as pointed by two yellow arrows in the image. Further enhancement of the displacement caused elongation of surface layer, furthermore the fracture of the surface layer occurred gradually.

The load-displacement curve (Fig. 6) shows that the tail of the curve is formed as a result of plastic deformation of the surface layer. The Influence of the zeolite content on the elongation of the surface layer is shown in Fig. 7. It is clearly seen that the surface layer is shorter with increasing content of zeolite.

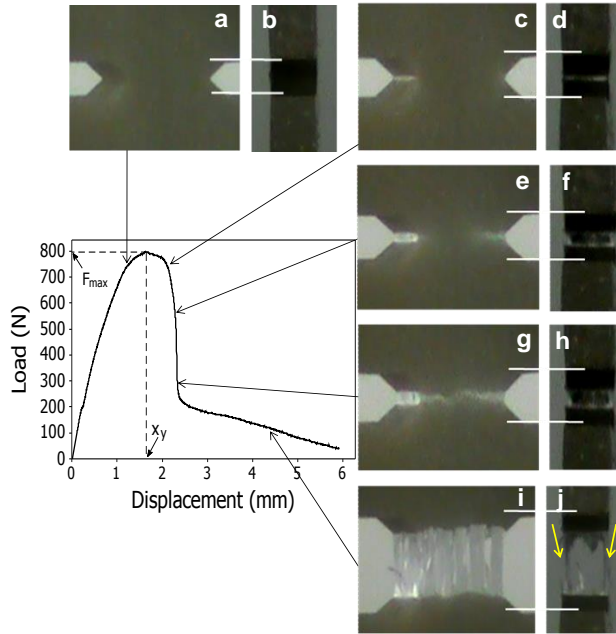


Fig. 6. The typical load-displacement curve and deformation behavior at ligament length region (taken from a specimen of 5 wt.% zeolite/HDPE with $\ell = 15$ mm). a, c, e, g, and i are the front view of the specimen at an angle of about 30 degrees; b, d, f, h, and j are side view showing typical fracture development through the ligament thickness.

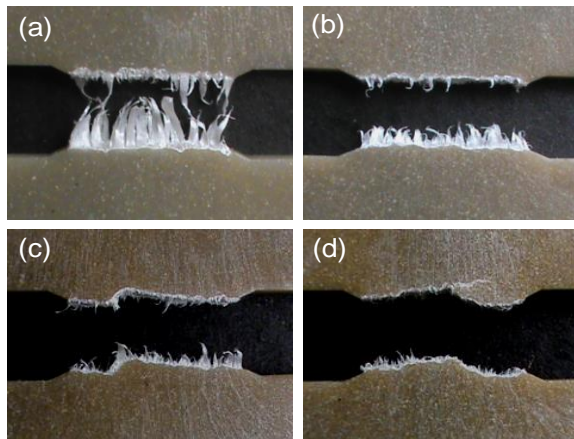


Fig. 7. Front view of the deformation behavior at ligament length region taken after DENT test for HDPE filled with zeolite of 5 wt.% (a), 10 wt.% (b), 15 wt.% (c), and 20 wt.% (d).

Based on energy partitioning work of fracture [18, 29, 31], the displacement at break (x_b) can be divided into the displacement for yielding (x_y) and displacement for necking-tearing (x_n). This relationship can be expressed by $x_b = x_y + x_n$. Furthermore, the plot of x_b , x_y , and x_n against ligament length is shown in Fig. 8. It revealed the linear relationship between the displacements (x_b , x_y , and x_n) and the

ligament length in all specimens tested. The elongation at break decreased with increasing the zeolite content. This indicates that the addition of zeolite restrict plastic deformation resulting in a decrease in ductility of matrix composites at higher zeolite content.

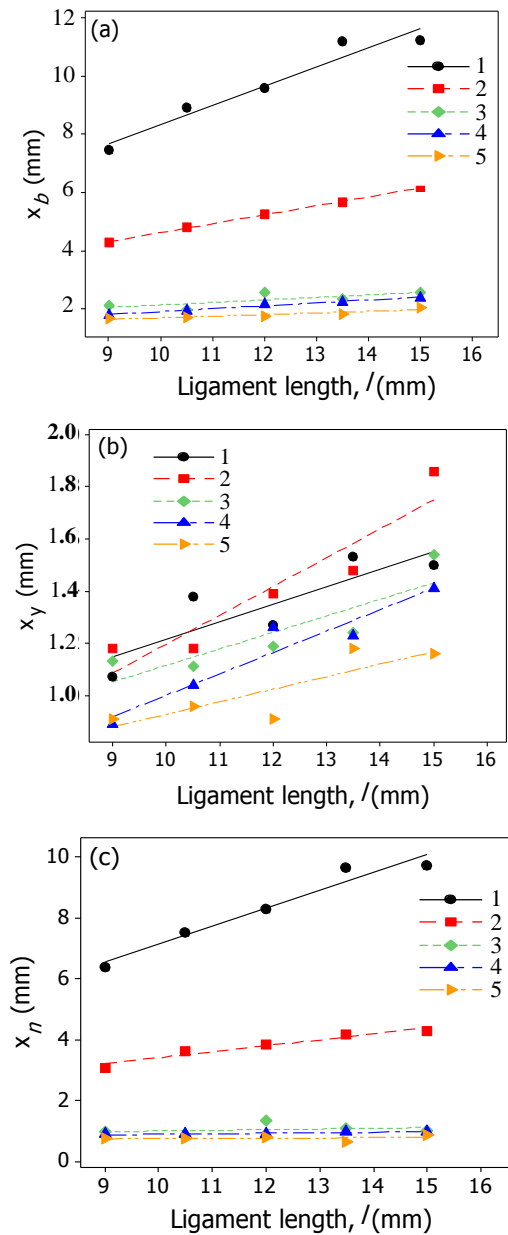


Fig. 8. The dependence of displacement on the ligament length: (a) displacement at break, (b) displacement of fully yielding, and (c) displacement of necking-tearing. Where 1 is pure HDPE, while 2, 3, 4, and 5 were the composites with zeolite content of 5 wt.%, 10 wt.%, 15 wt.%, and 20 wt.%, respectively.

In the whole tensile process of DENT specimens, it was clear that the elongation of the process of necking-tearing giving dominant contribution to the total extension of the material until the two halves of the specimen broken are not connected by surface layer. Under plane stress conditions, the linear relationship between x_b , x_y , and x_n with l can be expressed as [32-34]:

$$x_b = x_o + x_p l \quad (7)$$

$$x_y = x_{oy} + x_{py} l \quad (8)$$

$$x_n = x_{on} + x_{pn} l \quad (9)$$

where x_o , x_{oy} , and x_{on} were the crack opening displacement (COD) for whole process, yielding, and necking-tearing, respectively, x_p , x_{py} , and x_{pn} were the plastic contribution for whole extension, yielding, and necking-tearing, respectively. For their relationship, it was clear that the COD was the intercept value of the linear relationship at zero ligament length. Many researchers [35-37] have reported that empirically COD directly related to essential work of fracture. They expressed the empirical relationship as:

$$w_e = \gamma \sigma_y x_o \quad (10)$$

$$w_{e,y} = \gamma \sigma_y x_{oy} \quad (11)$$

$$w_{e,n} = \gamma \sigma_y x_{on} \quad (12)$$

where γ and σ_y are the plastic constraint factor and the yield stress which determined by uniaxial tensile test of dumbbell specimens, respectively. For the DENT specimens, the γ parameter is equal to 1.5 [27, 38]. The values of σ_y for zeolite content of 0 wt.%, 5 wt.%, 10 wt.%, 15 wt.%, and 20 wt.% were 8.89 MPa, 8.18 MPa, 7.9 MPa, 6.65 MPa, and 6.61 MPa, respectively [39]. The w_e , $w_{e,y}$, and $w_{e,n}$ parameters calculated based on empirical relationship with COD were shown in Table 1.

Table 1. The specific essential fracture work of the pre- and post-yield region estimated form EWF and COD.

Zeolite/HDPE (wt.%)	x_o (mm)	w_e (kJ/m²)	x_{oy} (mm)	w_{ey} (kJ/m²)	x_{on} (mm)	w_{en} (kJ/m²)
00/100	1.80	18.37	0.52	5.34	1.27	13.02
05/95	1.52	14.33	0.08	0.73	1.45	13.60
10/90	1.27	11.49	0.37	3.40	0.79	7.18
15/85	1.14	8.69	0.18	1.40	0.71	5.42
20/80	1.12	8.51	0.44	3.36	0.68	5.15

4. Conclusions

The deformation under quasi static loading in the zeolite-filled HDPE has been investigated both in the dumbbell and DENT specimens. The addition of zeolite resist plastic deformation of HDPE matrix which resulted in a decreased the total elongation of the composites. The composites with zeolite content of 20 wt.% on the ligament length of 9 and 10 mm were not in plane stress fracture even though the ligament length of specimens have been adapted to the requirements of plane stress fracture. This indicated that the deformation of that composites were

parallel to the plane, and their values do not depend on the distance perpendicular to the plane.

References

1. Ramakrishna, S.; Mayer, J.; Wintermantel, E.; and Leong, K.W. (2001). Biomedical applications of polymer-composite materials: A review. *Composites Science and Technology*, 61(9), 1189-1224.
2. Prein, J.; Assael, L.A.; Klotch, D.W.; Manson, P.N.; Rahn, B.A.; and Schilli, W. (1998). Manual of internal fixation in the cranio-facial skeleton, ISBN. 3-540-61810-4, Springer, New York.
3. Pavelic, K.; and Hadzija, M. (2003). *Medical applications of zeolites*. In: Auerbach, S.M, Carrado, K.M. and Dutta, P.K (Ed.): Handbook of zeolites sciences and technology. Marcel Dekker, New York, 1141-1173.
4. Pavelić, K.; Hadzija, M.; Bedrica, L.; Pavelić, J.; Dikić, I.; Katić, M.; Kralj, M.; Bosnar, M.H.; Kapitanović, S.; Poljak-Blazi, M.; Krizanac, S.; Stojković, R.; Jurin, M.; Subotić, B.; and Colić, M. (2001). Natural zeolite clinoptilolite: new adjuvant in anticancer therapy. *Journal of Molecular Medicine*, 78(12), 708-720.
5. Andronikashvili, T.; Pagava, K.; Kurashvili, T.; and Eprikashvili, L. (2009). Possibility of application of natural zeolites for medicinal purposes. *Bulletin of The Georgian National Academy of Sciences*, 3(2), 158-167.
6. Tomasovic-Canovic, M. (2005). Purification of natural zeolit e-clinoptilolite for medical application-extraction of lead. *Journal of the Serbian Chemical Society*, 70(11), 1335-1345.
7. Bedi, R.S.; Beving, D.E.; Zanello, L.P.; and Yan, Y.(2009). Biocompatibility of corrosion-resistant zeolite coatings for titanium alloy biomedical implants. *Acta Biomaterialia*, 5(8), 3265-3271.
8. Bedi, R.S.; Zanello, L.P.; and Yan, Y. (2009). Bone implants: osteoconductive and osteoinductive properties of zeolite MFI coatings on titanium alloys. *Advanced Functional Materials*, 19(24), 3856-3861.
9. Kaali, P.; and Czel, G. (2012). Single, binary and ternary ion exchanged zeolite as an effective bioactive filler for biomedical polymer composites. *Materials Science Forum*, 729, 234-239.
10. Bedi, R.S.; Chow, G.; Wang, J.; Zanello, L.; and Yan, Y.S. (2012). Bioactive materials for regenerative medicine: Zeolite-hydroxyapatite bone mimetic coatings. *Advanced Engineering Materials*, 14(3), 200-206.
11. Sanchez, M.J.; Gamero, P.; and Cortes, D. (2012). Bioactivity assessment of ZSM-5 type zeolite functionalized with silver or zinc. *Material Letters*, 74(1), 250-253.
12. Couldwell, W.T.; Chen, T.C.; and Weiss, M.H. (1994). Cranioplasty with the Medpor porous polyethylene flexblock implant. *Technical note. Journal of neurosurgery*, 81(3), 483-486.
13. Rubin, J.P.; and Yaremchuk, M.J. (1997). Complications and toxicities of implantable biomaterials used in facial reconstructive and aesthetic surgery: a comprehensive review of the literature. *Plastic and Reconstructive Surgery*, 100(5), 1336-1353.

14. Wellisz, T.; Dougherty, W.; and Gross, J. (1992). Craniofacial applications for the Medpor porous polyethylene flexblock implant. *Journal of Craniofacial Surgery*, 3(2), 101-107.
15. Zhang, Y.; and Tanner, K.E. (2003). Impact behavior of hydroxyapatite reinforced polyethylene composites. *Journal of material science: Material in medicine*, 14(1), 63-68.
16. Zhang, Y.; and Tanner, K.E. (2008). Effect of filler surface morphology on the impact behaviour of hydroxyapatite reinforced high density polyethylene composites. *Journal of Material Science: Material in Medicine*, 19(2), 761-766.
17. Mai, Y.W.; and Cotterell, B. (1984). The essential work of fracture for tearing of ductile metals. *International Journal of Fracture*, 24(3), 229-236.
18. Mai, Y.W.; and Cotterell, B. (1986). On the essential work of ductile fracture in polymers. *International Journal of Fracture*, 32(2), 105-125.
19. Karger-Kocsis, J.; Czigány, T.; and Moskala, E.J. (1997). Thickness dependence of work of fracture parameters of an amorphous copolyester. *Polymer*, 38(18), 4587- 4593.
20. Clutton, E. (2001). Fracture mechanics testing methods for polymers, adhesives and composites. *Elsevier*, Kidlington, UK.
21. Broberg, K.B. (1975). On stable crack growth. *Journal of the Mechanics and Physics of Solids*, 23(3), 215-237.
22. Cotterell, B.; and Reddel, J.K. (1977). The essential work of plane stress ductile fracture. *International Journal of Fracture*, 13(3), 267-277.
23. Mouzakis, D.E.; Papke, N.; Wu, J.S.; and Karger-Kocsis, J. (2001). Fracture toughness assessment of poly(ethylene terephthalate) blends with glycidyl methacrylate modified polyolefin elastomer using essential work of fracture method. *Journal of Applied Polymer Science*, 79(5), 842-852.
24. Yang, J.L.; Zhang, Z.; and Zhang, H. (2005). The essential work of fracture of polyamide 66 filled with TiO₂ nanoparticles. *Composites Science and Technology*, 65(2005), 2374-2379.
25. Karger-Kocsis, J. (1996). For what kind of polymer is the toughness assessment by the essential work concept straightforward? *Polymer Bulletin*, 37(1), 119-126.
26. Wu, J.; and Mai, Y.W. (1996). The essential fracture work concept for toughness measurement of ductile polymers. *Polymer Engineering and Science*, 36(18), 2275-2288.
27. Hashemi, S.; and Williams, J.G. (2000). Temperature dependence of essential and non-essential work of fracture parameters for polycarbonate film. *Plastics, Rubber and Composites*, 29(6), 294-302.
28. Purnomo; Soenoko, R.; Irawan, Y.S.; and Suprpto, A. (2014). Fracture behavior of zeolite-filled high density polyethylene based on energy partitioning work of fracture. *International Journal of Applied Engineering Research*, 9(24), 28737-28747.
29. Karger-Kocsis, J.; Czigány, T.; and Moskala, E.J. (1998). Deformation rate dependence of the essential and non-essential work of fracture parameters in an amorphous copolyester. *Polymer*, 39 (17), 3939-3944.

30. Mouzakis, D.E; Karger-Kockis, J; and Moskala, E.J. (2000). Interrelation between energy partitioned work of fracture parameters and the crack tip opening displacement in amorphous polyester films. *Journal of Materials Science Letters*, 19(18), 1615-1619.
31. Test protocol for essential work of fracture, vol. 28.ESIS Publication (2001).
32. Hashemi, S.; and O'Brien, D. (1993). The essential work of plane-stress ductile fracture of poly (ether-ether ketone) thermoplastic. *Journal of Materials Science*, 28(15), 3977-3982.
33. Hashemi, S. (1997). Fracture toughness evaluation of ductile polymeric films. *Journal of Materials Science*, 32(6), 1563-1573.
34. Bárány, T.; Czigány, T.; and Karger-Kocsis, J. (2010). Application of the essential work of fracture (EWF) concept for polymers, related blends and composites: a review. *Progress in Polymer Science*, 35(10), 1257-1287.
35. Arkhireyeva, A.; and Hashemi, S. (2004). Effect of temperature on work of fracture parameters in poly(ether-ether ketone) (PEEK) film. *Engineering Fracture Mechanics*, 71(4), 789-804.
36. Kuno, T.; Yamagishi, Y.; Kawamura, T.; and Nitta, K. (2008). Deformation mechanism under essential work of fracture process in polycyclo-olefin materials. *Express Polymer Letters*, 2(6), 404-412.
37. Costa, F.R.; Satapathy, B.K.; Wagenknecht, U.; Weidisch, R.; and Heinrich, G. (2006). Morphology and fracture behaviour of polyethylene/Mg-Al layered double hydroxide (LDH) nanocomposites. *European Polymer Journal*, 42(9), 2140-2152.
38. Hashemi, S. (2003). Work of fracture of high impact polystyrene (HIPS) film under plane stress conditions. *Journal of Materials Science*, 38(14), 3055-3062.
39. Purnomo; Soenoko, R.; Suprpto, A.; and Irawan, Y.S. (2015). Morphological and mechanical properties of natural zeolite-high density polyethylene composite. *International Journal of Applied Engineering Research*, 10(11), 28001-28012.